Polyhedron 140 (2018) 19–24

Contents lists available at ScienceDirect

Polyhedron

journal homepage: www.elsevier.com/locate/poly

$NaCa_4(BO_3)_3$: Ce, Dy, Eu phosphors for light emitting diode applications

Meiling Shi, Chaofeng Zhu *, Meimei Zhang, Meng Lu, Jianan Liu

Key Laboratory of Processing and Testing Technology of Glass & Functional Ceramics of Shandong Province, School of Materials Science and Engineering, Qilu University of Technology, Jinan 250353, PR China

ARTICLE INFO

Article history:
Received 26 September 2017
Accepted 16 October 2017
Available online 24 October 2017

Keywords:
Phosphor
Light emitting diode
Luminescence
Energy transfer
Rare earth ions

ABSTRACT

A series of Ce-, Dy-, and Eu-doped $NaCa_4(BO_3)_3$ phosphors for light emitting diodes (LEDs) applications were prepared using a high temperature solid state reaction method. These phosphors are investigated by X-ray diffraction, scanning electron microscopy, photoluminescence spectra, and Commission International de l'Eclairage chromaticity coordinates. It is found that crystals $Ca_3B_2O_6$ and $NaCa_4(BO_3)_3$ coexist in the phosphors, which can provide various local environments for the doped rare earth ions and affect the emission behavior of Ce^{3+}. The emission band splitting of Dy^{3+} is observed for the as-prepared phosphors. The energy transfer from Ce^{3+} to Dy^{3+} occurs in the Ce^{3+}/Dy^{3+} codoped phosphors. For Ce/Dy codoped phosphors, we find that the emission peak of Ce^{3+} moves to the longer wavelength with increasing the concentration of Ce^{3+} and Dy^{3+}. However, the emission peak of the Ce^{3+} single doped phosphor keeps nearly unchanged with the increase of Ce^{3+} content. The luminescence properties of the phosphors could be tailored effectively by varying the concentrations of the Ce, Dy, and Eu ions as well as the excitation wavelengths. The $NaCa_4(BO_3)_3$:Ce, Dy, Eu phosphors reported here demonstrate promising applications prospect in LEDs.

1. Introduction

Nowadays, white light-emitting diodes (W-LEDs) are regarded as a new generation lighting sources owing to their considerable merits of long lifetime, energy-saving, high efficiency, environmental friendliness, and so on [1–4]. Thus, LEDs are considered as a kind of significant lighting devices exhibiting high potential for the replacement of conventional lighting sources like incandescent and fluorescent lamps. Rare earth ions activated phosphors are currently used in LEDs [5,6]. Generally, the commercial phosphors converted white LEDs are fabricated using the blue LED (InGaN-based blue diode) chip and the yellow phosphor ($Y_3Al_5O_{12}:Ce^{3+}$ phosphor). However, a low color rendering index and a high correlated color temperature due to the deficiency of the red light component restrict the practical applications of the W-LEDs [7]. To solve these issues, a strategy of combining ultraviolet (UV) LED chip (the emission wavelength is in the range 300–400 nm) with tricolor (blue, green, and red) phosphors is employed for obtaining warm light W-LEDs. However, the respective emission reabsorption and different degradation rates of the respective primary phosphors caused the color aberration and low luminescence efficiency. In addition, the mixing of tricolor phosphors usually results in color imbalance at the higher operating temperature, high cost, and complicated fabrication process. To remove these disadvantages, some efforts have been focused on developing single-component white light emitting phosphors upon near ultraviolet (NUV) excitation. The single-component phosphors possess superior luminescence efficiency, color reproducibility and low manufacturing cost [8].

The phosphors for LEDs have been investigated for many hosts such as silicate, aluminate, nitride, phosphate, and borate, etc [9–16]. Rare earth doped borate phosphors have attracted great interest since they own the merit of low synthesis temperature and high thermal/chemical stability [17–20]. Dy^{3+} doped phosphors generally exhibit two intense emission bands located in the blue and yellow regions, which offers the possibility of obtaining near white light emission via the mixing of blue and yellow light. On the other hand, Ce^{3+} ions doped luminescent materials generally display a strong and broad 5d → 4f emission band, and Ce^{3+} ions can be introduced to the Dy^{3+}-doped phosphors to enrich the emission spectra and improve the luminescence property. Besides, Ce^{3+} ions can also be used as sensitizers to enhance the emission intensity of other active ions via the energy-transfer process. To acquire the superior quality of white light emission, more emission bands covering a broad visible region are expected. Herein we also introduce Eu ions into the Ce/Dy doped phosphors to compensate for the lack of red light emitting.

---

* Corresponding author. Fax: +86 531 89631226.
E-mail address: chaofengzhu@gmail.com (C. Zhu).

https://doi.org/10.1016/j.poly.2017.10.021
0277-5387/

Considering the emission colors of Ce, Dy, and Eu ions mentioned above, it is feasible to codope Ce/Dy/Eu into the phosphor host to realize white light emission. In this work, we investigate a series of Ce-, Dy-, and Eu-doped $NaCa_4(BO_3)_3$ phosphors. The crystal structure, the luminescence property, and the energy transfer from Ce^{3+} to Dy^{3+} in the phosphors are examined in detail. To the best of our knowledge, the $NaCa_4(BO_3)_3$: Ce, Dy, Eu phosphors for LEDs have not been further considered yet. The results of this work are scientifically intriguing and could also be technically important to the fabrication of LED devices.

2. Experimental procedure

The Ce-, Dy-, and Eu-activated $NaCa_4BO_3$ phosphors were synthesized via a high temperature solid state reaction technique. Analytical purity Na_2CO_3, $CaCO_3$, H_3BO_3, high purity (99.99%) CeO_2, Dy_2O_3, and Eu_2O_3 were weighed in the appropriate proportions and subsequently mixed and ground in an agate mortar. The mixed powders were then transferred into an alumina crucible, and pre-sintered in a furnace at 600 °C for 2 h in air to eliminate the water and decompose the carbonate. The pre-sintered samples were subsequently cooled down to room temperature and fully ground to form a homogeneous mixture. Then the mixture was re-sintered at a high temperature of 800 °C for 4 h in a reducing atmosphere attained using carbon granules. After sintering, the samples were cooled down naturally to room temperature in the furnace. The acquired sintered products were pulverized for further measurements. All the obtained samples are powders and show white appearance. The nominal molar compositions of the phosphors are as follows: $NaCa_{4\text{-}m}(BO_3)_3{:}mCe^{3+}$ ($m = 0.005$, 0.008, and 0.012), $NaCa_{3.95}(BO_3)_3{:}0.05Dy^{3+}$, $NaCa_{3.95\text{-}m}(BO_3)_3{:}mCe^{3+}$,0.05-$Dy^{3+}$ ($m = 0.005$, 0.008, 0.012), $NaCa_{3.995\text{-}n}(BO_3)_3{:}0.005Ce^{3+}$, nDy^{3+} ($n = 0.05$, 0.1, 0.15), and $NaCa_{3.945\text{-}x}(BO_3)_3$:0.005Ce, 0.05Dy, xEu ($x = 0.02$, 0.04, and 0.06).

The crystal phase identification was characterized by the X-ray diffractometer (XRD, Shimadzu, LabX XRD-6100) with Cu Kα radiation ($\lambda = 0.154$ nm). The morphology of the phosphors was examined using a field emission scanning electron microscope (FE-SEM, HITACHI, S-4800). The photoluminescence (PL) and photoluminescence excitation (PLE) spectra were recorded by a fluorescent spectrometer (Hitachi, F-4600) equipped with a Xe lamp as an excitation source. All measurements were performed using powder phosphors at room temperature with the same instrumental parameters.

3. Results and discussion

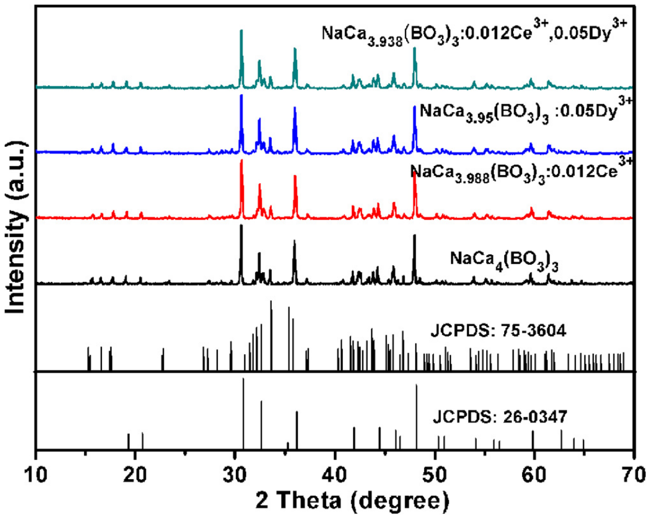

Fig. 1. XRD patterns of the samples. The standard XRD patterns of crystals $Ca_3B_2O_6$ (JCPDS No. 26-0347) and $NaCa_4(BO_3)_3$ (JCPDS No. 75-3604) are also shown for comparison.

Fig. 1 shows the XRD patterns of phosphors $NaCa_{3.988}(BO_3)_3{:}0.012Ce^{3+}$, $NaCa_{3.95}(BO_3)_3{:}0.05Dy^{3+}$, and $NaCa_{3.938}(BO_3)_3{:}0.012Ce^{3+},0.05Dy^{3+}$. The XRD profile of the host compound $NaCa_4(BO_3)_3$ is also included in Fig. 1 for comparison. Some sharp diffraction peaks can be observed, indicating that the crystalline phases exist in the samples. Compared to the standard XRD profiles of crystals $Ca_3B_2O_6$ (JCPDS No. 26-0347) and $NaCa_4(BO_3)_3$ (JCPDS No. 75-3604), as also shown in Fig. 1, all the XRD patterns of samples display the diffraction peaks of these two crystalline phases. So the as-prepared samples contain $Ca_3B_2O_6$ and $NaCa_4(BO_3)_3$ crystals. We can see that the XRD patterns of Ce^{3+}- and Dy^{3+}-doped phosphors are nearly identical to that of the host compound $NaCa_4(BO_3)_3$, indicating that the concentrations of the dopants (Ce^{3+} and Dy^{3+}) are too low to induce any significant changes to the host crystal structure.

SEM can be employed as a powerful tool to illustrate the morphologies of the phosphors [21]. Fig. 2 exhibits the SEM images of the samples shown in Fig. 1. We find that some phosphor particles are not uniform/regular in shape, which may be caused by the agglomeration of the particles during the sintering process. Simultaneously, the introduction of rare earth ions does not induce obvious changes in the particle shape and size. The size of particles of these phosphors is observed in the micron range around 4–10 µm, which can meet the demand for practical applications. It is reported that the phosphor particles in the micron range are suitable for fabrication of LED devices [8].

Fig. 3 presents the emission and excitation spectra of $NaCa_{3.988}(BO_3)_3{:}0.012Ce^{3+}$ phosphor. The emission spectra of this phosphor under three excitation wavelengths, which correspond to the excitation peaks (Fig. 3b), display the identical emission band shape and position except for the emission intensity. The variation of emission intensity correlates with the respective excitation peak intensity in Fig. 3b. The emission peak at ~394 nm and the emission shoulder at ~421 nm are observed in Fig. 3a. We also noticed that the excitation spectrum monitored at 394 nm shows three excitation bands (Fig. 3b). The emission and excitation of Ce^{3+} arise from the electronic transitions between the excited state 5d and ground state 4f and are highly affected by the coordinated surroundings [22,23], i.e., the emission and excitation behavior of Ce^{3+} ions is greatly dependent on the local structures around them. We have mentioned previously two crystalline phases, i.e., $Ca_3B_2O_6$ and $NaCa_4(BO_3)_3$, coexist in the phosphors, which can provide various local environments and enable multiple activator sites for Ce^{3+} ions. In the crystal $Ca_3B_2O_6$, the Ca^{2+} ions have one site with point symmetry C_2 and eight-coordinated by O^{2-} ions [24]. On the other hand, in $NaCa_4(BO_3)_3$ crystal, Ca^{2+} ions locate at three crystallographically different environments [25]. Ce^{3+} ions prefer to substitute Ca^{2+} ions due to the near ion radii of Ca^{2+} and Ce^{3+}. Thus, the emission centers (Ce^{3+}) are present in several ligand fields with respective crystal field strength. This may be responsible for the emission (~394 nm emission peak and ~421 nm emission shoulder) and excitation (three excitation bands) behavior of this phosphor.

The emission and excitation spectra of the Dy^{3+} single-doped $NaCa_{3.95}(BO_3)_3{:}0.05Dy^{3+}$ phosphor are shown in Fig. 4(a). The excitation spectrum monitored at the dominant emission at 480 nm exhibits several excitation bands peaking at ~325, 351, 365, and 388 nm, which correspond to the electronic transitions from ground state $^6H_{15/2}$ to the excited states $^6P_{3/2}$, $[^4I_{11/2},^4P_{7/2}]$, $[^4P_{3/2},^6P_{5/2}]$, and $[^4M_{21/2},^4I_{13/2}, ^4K_{17/2},^4F_{7/2}]$ [26–28], respectively.